CR-134189

FINAL REPORT

NAS 911640 (31-6055-A)

3-1-71 to 9-30-73

(NASA-CR-134189) UV PHOTOGRAPHY OF THE EARTH AND THE MOON Final Report, 1 Mar. 1971 - 30 Sep. 1973 (State Univ. of New York) 45 p HC $5.25 CSCL 14E

N74-17159

Unclas

G3/14 30453

UV PHOTOGRAPHY OF THE EARTH AND THE MOON

Tobias Owen

Department of Earth and Space Sciences, State University of New York,

Stony Brook, New York 11790

Table of Contents

1. Introduction

The fundamental aim of this experiment was the acquisition of ultraviolet photographs of the Earth and the moon that could be used to interpret similar imagery of Mars and Venus. It has been known for many years that both of these planets exhibit unusual appearances when photographed at wavelengths below 4500 Å.

Venus shows no markings whatever when viewed in visible light, a phenomenon that is in keeping with its immensely thick atmosphere and perpetual cloud cover, but in the near ultraviolet, the planet exhibits low contrast markings which vary in position and appearance with time (Figure 1). Evidence has recently been adduced in support of a four-day rotation period for these markings, but their nature is still not completely understood. Indeed, the basic composition of the clouds of Venus is the subject of great debate, although the idea that the upper clouds must consist primarily of sulfuric acid droplets as proposed by Young (1973) has become increasingly convincing. The presence of water ice in these clouds seems much less likely now than it did at the time of the inception of the present experiment (O'Leary 1970). At that time, it was hoped that imagery of the Earth at short wavelengths could be interpreted with the help of an _a priori_ knowledge of cloud composition and structure and the results used to help unravel the situation on Venus.

Mars has posed just the opposite problem from Venus--at wavelengths below 4500 Å, Mars shows very little detail, sometimes none at all, whereas at longer wavelengths, the surface is clearly visible (Figure 2). Occasionally observers have reported that this obscuration has lifted and the ground has become visible at the shorter wavelengths as well. Such events have been labeled "blue clearings" and led to the suggestion that the ultraviolet obscuration was caused by an atmospheric haze. Mariner 6 and 7 observations of Mars failed to find such a haze and lent support to the alternative view that ascribed the absence of detail on UV photographs to a simple lack of contrast between Martian surface features at these wavelengths. Once again, it was hoped that the imagery of known terrains on the Earth and the moon obtained on the present experiment would provide the data required to shed some light on this problem.

2. The Experiment

The basic requirements for the proposed experiment follow directly from the stated objectives. A suitable combination of camera, filters and film must be found to duplicate the conditions used to obtain ground-based photographs of Mars and Venus. The Apollo missions appeared to provide an ideal opportunity to carry out this project, since a wide variety of target distances and lighting conditions were provided, enabling a duplication of the phase angles and resolutions at which the planetary observations were made. The original conception involved carrying out the photography as part of several EVA's, but it quickly became apparent that this was not a practical procedure. Fortunately, two complete windows were still available in an uncoated state at the time the experiment was initiated. The absence of the coatings meant that the windows would permit transmission of UV radiation, as was verified by direct measurement (Table I). These windows were in the number 5 position in the Command Modules for Apollo 15 and 16. Plexiglass and cardboard shields were provided to protect the crew when the windows were not being used for photography. A standard 70 mm Hasselblad camera was mounted on a bracket behind the window as illustrated in Figure 3. The camera was equipped with a 105 mm Zeiss UV SONAR lens, the latter having excellent image-forming qualities over the wavelength range 2000 to 7000 Å. Eastman IIa-O emulsion was used on the 70-mm film base and a series of 4 filters was selected to isolate the wavelength regions of interest (Table II). Color photography for calibration could be obtained with the same set-up by substituting a camera back loaded with color film in place of the IIa-O film and using the UV-cutoff filter.

A diagram illustrating the transmission characteristics of the filters and the relative sensitivity of the IIa-O film is shown in Figure 4. The filters were selected to overlap with pass-bands commonly used for planetary photography from the ground, and to extend the wavelength range further into the UV (at 2650 Å) than is possible for ground-based observers. The ozone absorption cutoff is superimposed on Figure 4 to illustrate this point. It is evident that the pass-band of the 3050 Å filter is intersected by the ozone absorption edge. Hence when this filter is used from the ground (as it often is) it has an effective peak transmission shifted to 3200 Å. From space, this shift is absent, but the presence of the ozone absorption in the Earth's atmosphere means that in fact we will record very little scattered light from the planet at wavelengths below 3200 Å, so the effect is the same. In the case of the moon, a sharp cut-off does not exist, but the decrease in the lunar reflectivity with decreasing wavelength again implies an effective peak wavelength greater than 3050 Å for this filter (Pellicori 1972).

Of the filters listed in Table II, only the first two were successfully flown on Apollo 15; the 3050 Å filter did not pass flight qualifications and its nickel-sulfide element was not optically finished, while the 2650 Å filter had a long wavelength leak and produced multiple images as a result of reflections from the window. These two filters were rebuilt and remounted for the Apollo 16 flight. The 3050 Å filter was constructed as an epoxy-sealed sandwich in which the nickel-sulfide element was held between a Schott UG-2 filter and a piece of quartz. The result was stable, resistant to flight hazards and gave good optical performance. The 2650 Å filter was remade as an interference filter, since no other method for isolating a passband at this wavelength was available. The tighter specifications made it very difficult to produce, but the final product seemed acceptable, even after pre-flight testing.

The new 3050 Å filter performed very well on the Apollo 16 flight, but the new 2650 Å filter was apparently sufficiently transparent at $\lambda > 5500$ Å that radiation at these wavelengths swamped the contribution at 2650 Å despite the much lower sensitivity of the film at the longer wavelengths. Multiple images were again observed but appear not to have been the result of pinholes as originally suspected, but rather the product of the long wavelength light reflected internally within the filter itself. The defect in the design of the film-filter system was unfortunately not discovered until careful post-flight inspection of the filter was carried out.

3. Results

A listing of the imagery is given below (AS-15) and in Appendix 1 (AS-16). Color photography is available for each set of four images with the exception of the last set taken on Trans-Earth Coast (TEC) on Apollo 16, owing to premature stowage of the color magazine in that case. In the discussion that follows, we shall treat the two missions separately and then give some general conclusions and suggestions for additional work.

3.1 Apollo 15

The photographs for Apollo 15 were obtained according to the following plan:

Object	No. of sets
Earth from Earth orbit	1
Moon from TLC	1
Earth from TLC	3
Earth from Lunar Orbit	2
Moon from Lunar Orbit	2*
Earth from TEC	3
Moon from TEC	1

Here a "set" denotes two pictures taken through each of the three filters, or a total of six frames per set. The two sets of lunar photographs marked with an asterisk above included an extra set of two visible comparison frames at the end of the sequence to insure overlap with the UV images.

Images obtained with the visible and 3550 Å filters were of very high quality and remarkably similar in appearance. Examples are given in Figures 5 and 6. As mentioned above, these were the only two filters that performed satisfactorily on this mission. Unfortunately, the information that could be obtained from these observations was further limited by the fact that we did not get useful coverage of terrestrial land masses, thereby preventing an examination of ground contrast changes in the UV. An examination of the photographs that were obtained led to the following conclusions:

1. The surface of the Earth is still visible at 3550 Å but with somewhat reduced contrast.
2. No large scale changes in the visibility of aerosols occur at these two pass-bands (3550 Å and "visible").

These characteristics are radically different from those exhibited by Mars and Venus as described above. Both of these planets reveal their UV peculiarities at 3550 Å, so our inability to obtain high quality imagery at still shorter wavelengths does not vitiate this conclusion. Since the atmospheric pressure at the Earth's surface is two hundred times larger than that of Mars and our atmosphere is rich in aerosols, the visibility of surface detail at 3550 Å on Earth suggests that the lack of detail on Mars at this wavelength is not purely an atmospheric effect. In other words, the idea of a "blue haze" in the Martian atmosphere finds no support in the form of a terrestrial analog. Consequently, the class of theories that explain the lack of detail on UV photographs of Mars in terms of an intrinsic loss of surface contrast at short wavelengths seems more reasonable based on these data.

3.2 Apollo 16

It was decided to forego the orbital imagery of the Earth on this mission in favor of increased near-Earth and near-moon coverage. Despite the additional photographs, however, it still was not possible for us to obtain images of land masses on the Earth, owing to the vagaries of terrestrial weather patterns and the tight schedules of the flight crew. We were able to extend the wavelength coverage as compared with Apollo 15, and fortuitously captured a most interesting atmospheric effect at the end of the mission.

3.2.1 Earth Coverage

A comparison of the appearance of the Earth at effective wavelengths of 3200 Å and 4600 Å is given in Figures 7 and 8, respectively. At first glance, one sees very little difference between the appearance of our planet at these two wavelengths. We are looking at the Pacific Ocean, with Baja California just disappearing at the terminator. The detail one sees is thus primarily cloud patterns against the ocean background. Close inspection of second generation positives reveals that low altitude clouds and air-sea boundaries have almost entirely disappeared from the image obtained at the shorter wavelength (Figure 7). The diffusely reflected image of the sun present on the 4600 Å picture (Figure 8) is also missing from Figure 7. These results are entirely consistent with predictions from elementary scattering theory, which suggest a marked increase in the brightness of a planet's atmosphere will occur with decreasing wavelength.

Using simple Rayleigh scattering we can compare the extinction coefficient β at 4600 Å and 3200 Å. We define β from the relation for the decrease of intensity Io of a beam of light over a path L: $I = Io\ e^{-\beta L}$. We then find $\beta_{3200}/\beta_{4600} = 11.21/2.47 = 4.53$ (Van de Hulst 1952). This is the difference between an optical depth of 0.2 at 4600 Å and 0.9 at 3200 Å. Since an optical depth of unity is commonly regarded as opaque, we see that Rayleigh scattering alone can essentially explain the observed effects, although there is undoubtedly a contribution from aerosols.

Unfortunately, these results tell us nothing about Mars and Venus. In the case of Mars, we would need to examine the wavelength dependence of the surface contrast observed at various regions on a land mass, which we were unable to photograph as mentioned above. We can only confirm the impression reached on Apollo 15 that the Martian atmosphere is probably not exclusively responsible for the loss of detail on that planet's surface at wavelengths below 4500 Å. For Venus, we need to look much higher in our atmosphere for possible analogies to the Cytherean ultraviolet clouds. The 2650 Å filter was designed for this purpose but did not perform well enough to permit such an investigation to be carried out.

However, by chance some imagery was obtained that may have a bearing on the Venus atmosphere. The final TEC sequence caught a bright "flash" at the limb of the crescent Earth (Figure 9). It is a pity that we do not have the color photography to provide an independent record of this effect in a form that might be easier to interpret in terms of available meteorological data. However, we do have another independent observation--a visual record by the astronauts as indicated by the following exchange from the voice transcript (Apollo 16 Air-to-

Ground Voice Transcription, p. 2041, Tape 172/1).

10-23-15-46 CDR "Hank, we got the Earth out of window 5. It's a very thin crescent and the subsolar point is-- spectacularly bright."

10-23-15-59 CC "Sounds great."

10-23-16-01 CDR "It looks great, I'll tell you."

Inspection of second generation copies indicates that this surge of brightness is caused by a reflection from an irregularly shaped area surrounded by a featureless haze. The bright spot is invisible on the frames shot at 3200 Å, partially apparent at 3550 Å, and strongest at 4600 Å. At the extreme limb, we are looking at very large optical depths owing to the large angles of incidence and observation. Thus the reflecting surface may simply not be brightly illuminated or visible at the shortest wavelength because of its relative proximity to the planet's surface.

In fact, the astronauts could not see the "subsolar" point, the bright area must occur at the specular reflection point where the angle between the incident sunlight and the local normal is equal to the angle between the normal and the line of sight to the Command Module. This geometry is illustrated in the line drawing in Figure 10. What was the cause of this bright flash? Our original interpretation was that the effect was the result of sunlight reflected either from an open body of water or from ice crystals in local cloud cover (Owen 1972). It was not possible to distinguish between these alternatives at the time because we did not know the exact coordinates of the subspacecraft position nor did we have suitable meteorological records available. Both of these problems have been remedied so we can now pursue this investigation with greater rigor.

The first step is to determine the latitude and longitude of the specular reflection point. The position of the command module at the mid-point of the photographic sequence was determined by Mr. J. W. Simpson from orbital data, astronaut interviews and the voice tapes. The actual elapsed time (AET) at the midpoint of the sequence was $262^h\ 53^m$, corresponding to GMT April 27, 1972 $16^h\ 47^m$. This information enables us to find the subsolar coordinates from the <u>American Ephemeris and Nautical Almanac</u> for 1972.

In order to determine the latitude and longitude of the specular reflection point, we make use of the relation

1) $r \sin (\phi-2a) = R \sin (\phi-a)$

which may be derived by inspection of Figure 10.

r = 23,221 nautical miles, the distance of the command module from the Earth and R = 3442 nautical miles, the radius of the Earth. The phase angle ϕ can be derived from the subspacecraft and subsolar latitudes and longitudes using spherical trigonometry. The relevant coordinates are as follows:

subsolar:	14° 01' North
	71° 40' West
subspacecraft:	30° 49' South
	78° 56' East

Using these values, one finds that ϕ = 152° 45'. We can now solve equation (1) for the angle a, since all other quantities are known. We find a = 72° 20'. This angle can then be subtracted from ϕ and the coordinates of the resulting point on the Earth's surface can be derived with the sine and cosine relations of spherical trigonometry. The result is

Specular Reflection Point	4° South
	7° East

In view of various uncertainties involved in this calculation, it is estimated that the precision of these coordinates is no better than ±1°, but this is perfectly adequate for our purposes. Consulting an Atlas, we find that the specular reflection point was in or over the South Atlantic just off the west coast of Africa. We are now in a position to investigate weather records to determine local conditions in the area immediately surrounding this location at the time of the Apollo 16 photography.

Unfortunately, we do not have the exact information we would like since the Apollo photography occurred when this location was very close to the terminator, poorly placed for satellite surveillance. We do have ESSA photography obtained near local noon on the 27th and 28th of April, however, giving some idea of local conditions before and after the event depicted in Figure 9. We also have ATS photography obtained throughout the day, but with our region very foreshortened on the eastern horizon. Inspection of both data sets reveals that there were clouds in the area, although the main concentration appears to have been slightly farther north and west than the specular reflection point derived above. A sample photograph is reproduced as Figure 11.

Inspection of a large number of other Apollo and ATS photographs of the Earth failed to show an identical instance of specular reflection, despite the fact that on many occasions the oceans were exposed at the reflection point. A typical example from Apollo 11 is shown in Figure 12 (cf. Fig. 8). A diffuse image of the sun is seen, owing to the fact that the surface of the ocean is not smooth. A case of near-specular reflection superimposed on the diffuse brightening is shown in Figure 13 from the Apollo 13 mission. This appears to be similar to the effect captured in the present mission, although the phase angle is somewhat smaller. Our interpretation of both of these cases is the same, viz., the reflection is thought to arise from ice crystals formed as hexagonal plates (Mason 1971) and falling slowly in parallel alignment. This is a comparatively rare phenomenon apparently, since it is not prevalent in the meteorological satellite records (V. Suomi, private communication), nor is it seen often from airplanes or mountains. We did not observe it in the Apollo 15 imagery. However, it has been included by Minnaert (1954) in his compendium of natural optical phenomena. I have personally observed specular reflection from clouds only once, on a transcontinental flight in February 1973. On that occasion, the reflection came from a thin mist overlying thicker, cumuliform clouds. Unfortunately we have no local records of cloud observations over the west coast of Africa to provide "ground truth," but in the absence of reasonable alternatives, this is the best interpretation of Figure 9 that we can develop.

What makes this observation interesting for the present program is the fact that such an effect has never been observed on photographs or by direct observations of Venus, despite the fact that this planet passes through similar phase angles as viewed from the Earth (cf. Fig. 1).

Several investigators have looked very carefully into the possibility of detecting ice crystals in the Venus clouds by means of the 22° halo they would produce (e.g., O'Leary 1970). In this case the hexagonal crystals would be elongated prisms rather than flat plates. The observations have always been rather marginal, with no clear evidence for ice detection. It would appear that an attempt to look for specular reflection in the atmosphere of Venus might be a more more sensitive test for the presence of ice and that the absence of such phenomena would place rather severe constraints on the possibility that hexagonal ice crystals are an important component of the visible cloud deck of that planet. This is of course consistent with recent polarimetric and spectroscopic results that appear to indicate that the uppermost cloud layer consists of sulfuric acid droplets (Hansen and Arking 1971, Young 1973).

3.2.2 Lunar Coverage

The appearance of the moon at effective wavelengths of 3050 Å and 4600 Å is illustrated in Figures 14 and 15. Once again, there is little apparent difference between images obtained at these two wavelengths, certainly nothing as dramatic as the loss of contrast that occurs on Mars (Figure 2). The hypothesis that contrast on the moon might disappear at short wavelengths rests on the idea that the differenc in appearance of dark and light areas is caused by different translucencies in the particles making up the maria and the terrae. At sufficiently short wavelengths, it is suggested that absorption becomes complete and only externally scattered light is visible, thereby eliminating any contrast between the two types of terrain (Pellicori

1971). It may be that we have simply not reached short enough wavelengths for the effect to become apparent, or perhaps some modifications in this interpretation of the observations are required.

It would be especially interesting to detect and analyse this loss of contrast on the moon, if it does occur, since we are learning about the properties of the lunar soil from direct analysis and thus should be able to provide a better model for Martian soil from a detailed comparison of the optical properties of Mars and the moon in the near UV. Similar photometric data on the planet Mercury should soon become available from the MVM mission.

4. Conclusions and Recommendations

It should be evident from the foregoing that this experiment has raised more questions than it has answered. The UV imagery of the Earth and moon have not been as instructive in the interpretation of observations of Mars and Venus as had been hoped. Our results support models for the lack of surface contrast on Mars at short wavelengths that do not involve atmospheric effects, but we have not been able to demonstrate a clear analog of the Martian phenomenon on either the Earth or the moon. Our search for possible high altitude cloud effects on Earth that might be similar to the UV clouds on Venus was frustrated by the poor performance of our 2650 Å filter. On the positive side, the experiment did record an unusual case of specular reflection from terrestrial clouds near the sunset terminator. The absence of this effect in the extensive literature recording observations of Venus adds further weight to arguments against the presence of ice crystals in the upper cloud layers of that planet's atmosphere.

One clear recommendation that emerges from the present exercise is to have more flexibility for the crew in selecting times to carry out the experiment. This would permit photography of "targets of opportunity" including the acquisition of images of suitably located and unobscured terrain. Trying to study ground contrast on a planet whose surface is 75% ocean and whose atmosphere exhibits roughly 50% cloud cover is not really a feat that can be pre-programmed unless very extensive photography is planned. A second difficulty we encountered was the construction of a suitable filter for wavelengths below 3000 Å. This is not an insuperable problem, but one that requires more care and may lead to awkwardly long exposure times for Earth photography owing to the planet's low albedo in this spectral region and the low transmittance of a suitably blocked filter. This in turn suggests a special camera for this experiment. Despite these handicaps, a useful set of data was obtained and the basic technique has been shown to be effective. One hopes that future photography from space will continue to include studies in the ultraviolet.

In this connection, it is worth pointing out that the Mariner 10 mission to Venus and Mercury currently underway includes a 3750 Å filter for use with the vidicon experiment. Some imagery of the Earth and moon has already been obtained with this instrument and it will be most interesting to compare these results with those obtained on the Apollo 15 and 16 missions. But the most intriguing comparison will be between the multi-color imagery of Mercury with the present work on the moon, since the apparent gross similarity between the photometric properties of the moon and Mercury is well known (McCord and Adams 1972). Does this similarity hold at high spatial resolution? Does contrast disappear on Mercury at longer wavelengths than on the moon? We will soon know the answers, since Mercury encounter for this mission occurs in March 1974.

Looking further ahead, it is anticipated that the present data set will also provide a useful reference for interpretation of UV imagery of the satellites of Jupiter and Saturn planned for the end of this decade. As a participant in the imaging experiment for this mission, I will be in a position to make a direct comparison between the two groups of ultraviolet images and I anticipate that this will be a very productive exercise.

Acknowledgements

It would have been impossible to carry out this experiment without the dedicated support of S. N. Hardee and J. W. Simpson of the Manned Spacecraft Center. Processing of the film, sensitometry and the production of many positive prints were all carried out with care and dispatch under the direction of N. T. Lamar. Figures 1 and 2 were generously provided by B. A. Smith from the collection at New Mexico State University. The cooperation and innovation exhibited by the Apollo 15 and 16 flight crews, especially A. Worden and K. Mattingly, was very gratifying. Discussions with S. Pellicori, R. Krauss, A. Collins, and V. Suomi were very helpful to the interpretation of the results.

References

Hansen, J. E. and Arking, A. 1971, Science, **171**, 669.

Mason, B. J. 1971, The Physics of Clouds, 2nd ed. (Oxford: Clarendon Press) p. 245.

McCord, T. B. and Adams, J. B. 1972, Science, **178**, 746.

Minnaert, M. 1954, The Nature of Light and Color in the Open Air (translation by H. M. Kremer-Priest, revision by K. E. Brian Jay: Dover, New York), p. 203.

O'Leary, B. 1970, Icarus, **13**, 292.

Owen, T. 1972, Apollo 16 Preliminary Science Report (NASA SP-315: Washington, U.S. Superintendent of Documents), Chap. 17.

Pellicori, S. F. 1971, Appl. Optics, **10**, 270.

Pellicori, S. F. 1972 (private communication).

van de Hulst, H. C. 1952 in The Atmospheres of the Earth and Planets, ed. G. P. Kuiper and B. M. Middlehurst (Chicago: University of Chicago Press), pp. 49-56.

Young, A. T. 1973, Icarus, **18**, 564.

Table I

The Ultraviolet Transmission of the Command Module Window

Wavelength	Transmission	
	Apollo 15	Apollo 16
2680 Å	68%	85%
3250	87	90
3750	88	90
4500	88	90
6300	89	91

Table II

The Transmission Characteristics of the Filters

Filter Designation	Passband, Å
UV cut-off	$\lambda > 4000$
3550	3150 to 3900
3050	2700 to 3300
2650	2550 to 2700

Figure Captions

1. Venus photographed at New Mexico State University April 6, 1966 at an effective wavelength of 3600 Å.
2. Mars photographed at New Mexico State University September 25, 1971 at the following effective wavelengths: (A) 3200 Å, (B) 3600 Å, (C) 4100 Å, (D) 4500 Å, (E) 5000 Å, (F) 5500 Å, (G) 6500 Å, (H) 8000 Å. The A, B, and D passbands are comparable to those of the filters used in the present experiment. The strong wavelength dependence of the surface contrast should be noted.
3. The Hasselblad Camera with filter wheel in place mounted in position behind window 5.
4. The filter and film characteristics for the UV photography experiment. The curve of the ozone absorption coefficient is included for reference.
5. Earth at 4600 Å. TLC, Apollo 15, f/4.3, 1/500. (AS15-99-13415).
6. Earth at 3750 Å. TLC, Apollo 15, f/4.3, 1/250. (AS15-99-13414).
7. Earth at 3200 Å. TLC, Apollo 16, f/4.3, 1/125. (AS16-131-20106).
8. Earth at 4600 Å. TLC, Apollo 16, f/8, 1/500. (AS16-131-20100).
9. Earth at 4600 Å. TEC, Apollo 16, f/8, 1/500. (AS16-131-20181).
10. Geometry at the Earth for specular reflection at point S. Command Module at point CM, distance r from Earth center. CM' is the position of CM reflected around the line SE so the angle CM'-E-S equals the angle CM-E-S which is the angle "a". The dashed lines illustrate the triangles needed for the derivation of equation (1).

11. Earth seen by the ATS 3 at 12:09 UT April 27. Note patchy cloud mass off west coast of Africa near equator.

12. Earth in color, Apollo 11. (AS11-6674).

13. Earth in color, Apollo 13. (AS13-8602).

14. The moon at 3050 Å. TEC, Apollo 16, f/4.3, 1/60. (AS16-131-20165).

15. The moon at 4600 Å. TEC, Apollo 16, f/4.3, 1/500. (AS16-131-20158).

Appendix 1

Apollo 16 Exposures

The following pages of information regarding Apollo 16 UV imagery were compiled by J. W. Simpson. They are included here for reference purposes.

COPY FOR DR. OWEN

5th EXPOSURE IS MID-SEQ. TIME (SEQUENCE)
LAUNCH 4/16/72 AT 17:54:00 GMT
11:54:00 CST
LOI = 74:24:41.8
(SEQUENTIAL)

EXPERIMENT S-177 (UV PTG ⊕ & ☾) FILM DATA - AP-16

PAGE No 1

SCHEDULED PHOTO NO. MPD		TARGET No. MPD	PHOTO YES/NO	ACTUAL PHOTO No.	TARGET / SUBJECT	λ (Å) PASS BAND CENTER	f/STOP	EXPOSURE (SEC)	TRUE IMAGE	IMAGE DIAM.	GET SEQUENCE TIME	GMT SEQ TIME	CM-DISTANCE FROM THE ⊕	⊕ SUB POINT	SUB-SPACECRAFT φλ AT SEQUENCE TIME	IMAGE QUAL.	AS16 FRAME No.
PHOTO SEQUENCE NO. 1	1	1	YES	1	⊕ DISC	3050 Å	4.3	1/125	YES		[illegible]		CM-D-⊕-35,460			E	AS16-131-20,100
	2	1	"	2	" "	3050 "	4.3	1/125	"							E	AS16-" -20,101
	3	1	"	3	" "	2600 "	4.3	2.0	" DOUBLE							P	AS16 -" 20,102
	4	1	"	4	" "	2600 "	4.3	2.0	" DOUBLE							P	AS16 - " -20,103
	5	1	"	5	" "	3750 "	4.3	1/125	"	19.1 mm	07:22:30	4/17/72 07-16-30Z	35,460 NM	λ 161°E.	λ 130° 44' WEST φ 30° 28' NORTH	E	CEX-AS16-118-11337 (COLOR) AS16-131-20,104
	6	1	"	6	" "	3750 "	4.3	1/125	"							E	AS16-131-20,105
	7	1	"	7	" "	>4000 "	8.0	1/500	"							E	AS16-131-20,106
	8	1	YES	8	⊕ DISC	>4000 Å	2.0	1/500	YES		[illegible]					E	AS16-131-20,107
NO. 2	9	2	YES	9	⊕ DISC	3000 Å	5.6	1/125	YES		[illegible]					G	AS16-131-20,108
	10	2	"	10	" "	3000 "	5.6	1/125	"							G	AS16-131-20,109
	11	2	"	11	" "	2600 "	5.6	1/25	"							P-G	AS16-131-20,110
	12	2	"	12	"	2600 "	5.6	1/25	"							P-G	AS16-131-20,111
	13	2	"	13	" "	3750 "	5.6	1/250	"	11.6 mm	[illegible]	4/17/72 [illegible]	60,789 NM	[illegible]	λ 139° 54' [illegible] φ 25° 24' [illegible]	G	CEX-AS16-118-[illegible] (COLOR) AS16-131-20,112
	14	2	"	14	" "	3750 "	5.6	1/250	"							G	AS16-131-20,113
	15	2	"	15	" "	>4000 "	8.0	1/500	"							G	AS16-131-20,114
	16	2	YES	16	⊕ DISC	>4000 Å	8.0	1/500	YES		[illegible]					G	AS16-131-20,115
NO. 3	17	3	YES	17	⊕ DISC	3000 Å	4.3	1/125	YES		[illegible]					G	AS16-131-20,116
	18	3	"	18	" "	3000 "	4.3	1/125	"							G	AS16-131-20,117
	19	3	"	19	" "	2600 "	4.3	2.0	"							P-G	AS16-131-20,118
	20	3	"	20	" "	2600 "	4.3	2.0	"							P-G	AS16-131-20,119
	21	3	"	21	" "	3750 "	4.3	1/125	"	6.45 mm	[illegible]	4/17/72 [illegible]	116,625 NM	[illegible]	λ 91° 25' [illegible] φ 25° 12' NORTH	G	CEX-AS16-118-[illegible] (COLOR) AS16-131-20,120
	22	3	"	22	" "	3750 "	4.3	1/125	"							G	AS16-131-20,121
	23	3	"	23	" "	>4000 "	8.0	1/500	"							G	AS16-131-20,122
	24	3	YES	24	⊕ DISC	>4000 Å	8.0	1/500	YES		[illegible]					G	AS16-131-20,123

REMARKS

Sequence No. 1:
MID-SEQUENCE TIME
07-22-30 AET 4/17/72
(ALL SEQUENCE AVERAGES SHOWN IN THE 5th FRAME SET OF EACH SEQUENCE)

⊕ VIEW COVERAGE
WESTERN & CENTRAL AMERICA
CENTRAL AMERICA
N.W. PART OF SOUTH AMERICA
PACIFIC OCEAN

LAUNCH: 4/16/72 at 11:54:00 CST
GMT or 17-54-00 Z

LOI: 74:24:41.8 AET
TRANS LUNAR COAST (TLC)

Sequence No. 2:
⊕ VIEW COVERAGE
ALL OF AUSTRALIA
NORTH, CENTRAL, & SOUTH PACIFIC AREAS
SOUTH EAST ASIA JAPAN
NORTH EAST ASIA

TLC

Sequence No. 3:
⊕ VIEW COVERAGE
MOST OF NORTH AMERICA
CENTRAL AMERICA
N.W. PART OF SOUTH AMERICA
PACIFIC-WEST OF AMERICAS

TLC

J.W.S.
8/11/72

EXPERIMENT S-177 (UV PTG ⊕ & ☾) FILM DATA - AP-16

SCHEDULED PHOTO NO. MRD		TARGET No. MRD	PHOTO YES/NO	ACTUAL PHOTO No. (SEQUENTIAL)	TARGET / SUB TEST	λ (Å) PASS BAND CENTER	f/ STOP	EXPOSURE	TRUE IMAGE	IMAGE DIAM.	GET SEQUENCE TIME	GMT SEQ TIME	CM-DISTANCE FROM THE ⊕	⊙ SUB POINT	SUB-SPACECRAFT Øλ AT SEQUENCE TIME	IMAGE QUAL.	AS16-FRAME No.	REMARKS
NO. 4	25	4	YES	25	⊕ DISC	3050 Å	5.6	[illegible]	YES							G	AS16-131- 20,124	⊕VIEW COVERAGE AFRICA ARABIA INDIAN OCEAN AUSTRALIA
	26	4	"	26	" "	3050 Å	5.6	[illegible]	"							G	AS16-131 20,125	TLC
	27	4	"	27	" "	2600 Å	5.6	[illegible]	"							P	AS16-131 20,126	
	28	4	"	28	" "	2600 Å	5.6	[illegible]	"							P	AS16-131 - 20,127	
	29	4	"	29	" "	3750 Å	5.6	[illegible]	"	[illegible]	[illegible]	[illegible]	166,797 NM	λ 160°W	λ 072° [illegible] φ 23° [illegible]	G	CEV-AS16-119-[illegible] / AS16-131 - 20,128	
	30	4	"	30	" "	3750 Å	5.6	1/250	"							G	AS16-131 - 20,129	
	31	4	"	31	" "	>4000 Å	8.0	[illegible]	"							G	AS16-131 20,130	
	32	4	YES	32	⊕ DISC	>4000 Å	8.0	[illegible]	YES							G	AS16-131. - 20,131	
NO. 5-A	33	5-A	YES	33	☾ DISC SET 1	3050 Å	4.3	1/60	NONE							N/A	AS16-131 - 20,132	ERROR IN SPACECRAFT POINTING. REFLECTIONS FROM NEARBY BRIGHT OBJECT, BUT NO OBJECT IN CAMERA FOV.
	34	5-A	"	34	" "	3050 Å	4.3	1/60	"							N/A	AS16-131 - 20,133	TLC
	35	5-A	"	35	" "	2600 Å	4.3	1/15	"							N/A	AS16-131 - 20,134	PRE-LOI
	36	5-A	"	36	" "	2600 Å	4.3	[illegible]	"							N/A	AS16-131 - 20,135	(8 FRAMES WITHOUT IMAGES)
	37	5-A	"	37	" "	3750 Å	4.3	1/60	"	N/A	[illegible]	[illegible]	193,284 NM	λ 036°W.	λ 052° [illegible] EAST φ 22° 37' NORTH	NONE	No EQUIVALENT COLOR PRINT AS16-131 - 20,136	
	38	5-A	"	38	" "	3750 Å	4.3	1/60	"							N/A	AS16-131 - 20,137	
	39	5-A	"	39	" "	>4000 Å	4.3	1/250	"							N/A	AS16-131 - 20,138	
	40	5-A	YES	40	☾ DISC SET 1	>4000 Å	4.3	1/250	NONE							N/A	AS16-131 - 20,139	
NO. 5 B	41	5-B	YES	41	☾ DISC SET 2	3050 Å	5.6	1/60	NONE							N/A	AS16-131 - 20,140	ERROR IN SPACECRAFT POINTING. REFLECTIONS FROM NEARBY BRIGHT OBJECT, BUT NO OBJECT IN CAMERA FOV.
	42	5-B	"	42	" "	3050 Å	5.6	1/60	"							N/A	AS16-131 - 20,141	TLC
	43	5-B	"	43	" "	2600 Å	5.6	1.0	"							N/A	AS16-131 - 20,142	PRE-LOI
	44	5-B	"	44	" "	2600 Å	5.6	1.0	"							N/A	AS16-131 - 20,143	(8 FRAMES WITHOUT IMAGES)
	45	5-B	"	45	" "	3750 Å	5.6	1/60	"	N/A	[illegible]	[illegible] 19-37-30	193,413 NM	N/A	λ 049° [illegible] EAST φ 23° 37' NORTH	NONE	No EQUIVALENT COLOR PHOTO AS16-131 - 20,144	
	46	5-B	"	46	" "	3750 Å	5.6	1/60	"							N/A	AS16-131 - 20,145	
	47	5-B	"	47	" "	>4000 Å	5.6	1/250	"							N/A	AS16-131 - 20,146	
	48	5-B	YES	48	☾ DISC SET 2	>4000 Å	5.6	1/250	NONE							N/A	AS16-131 - 20,147	

J.W.S.
8/11/72

EXPERIMENT S-177 (UV PTG ⊕ & ☾) FILM DATA - AP-16

SCHEDULED PHOTO NO. MRD		TARGET No. MRD	PHOTO YES/NO	ACTUAL PHOTO No. (SEQUENTIAL)	TARGET / SUBJECT	λ (Å) PASS BAND CENTER	f/ STOP	EXPOSURE	TRUE IMAGE	IMAGE DIAM.	GET SEQUENCE TIME	GMT SEQ TIME	CM-DISTANCE FROM THE ⊕	⊙ SUB POINT	SUB-SPACECRAFT φλ AT SEQUENCE TIME	IMAGE QUAL.	AS16- FRAME NO.
NO. 6	49	6	YES	49	☾ MARIA	3050 Å	4.3	1/60	YES							[illegible]	AS16-131-20,148
	50	6	"	50	" "	3050 Å	4.3	1/60	"							G	AS16-131-20,149
	51	6	"	51	" "	2600 Å	4.3	1/5	"							E	AS16-131-20,150
	52	6	"	52	" "	2600 Å	4.3	1/5	"							E	AS16-131-20,151
	53	6	"	53	" "	3750 Å	4.3	1/60	"	25 mm	171:10:[illegible]	4/[illegible]/72 [illegible]	206,[illegible] NM (APPROX)	N/A	λ 001° 00' WEST φ 13° 30' NORTH	F	NO EQUIVALENT COLOR PHOTO AS16-131-20,152
	54	6	"	54	" "	3750 Å	4.3	1/60	"							P	AS16-131-20,153
	55	6	"	55	" "	>4000 Å	5.6	1/250	"							E	AS16-131-20,154
	56	6	YES	56	☾ MARIA	>4000 Å	5.6	1/250	YES							E	AS16-131-20,155
No. 6 EXTRA	NOT SCHED.	6	YES	57	NOT SCHED.	Å	?	?	YES							G	AS16-131-20,156
	NOT SCHED.	6	YES	58	NOT SCHED.	Å	?	?	YES							G	AS16-131-20,157
NO. 10-A	57	10A	YES	59	☾ DISC	3050 Å	4.3	1/60	YES							E	AS16-131-20,158
	58	10A	"	60	" "	3050 Å	4.3	1/60	"							E	AS16-131-20,159
	59	10A	"	61	" "	2600 Å	4.3	1/15	"							F	AS16-131-20,160
	60	10A	"	62	" "	2600 Å	4.3	1/15	"							F	AS16-131-20,161
	61	10A	"	63	" "	3750 Å	4.3	1/60	"	NO ⊕	201:13:42	4/25/72 03-47-42	213,067 NM.	N/A	λ 025° 00' WEST φ 03° 51' SOUTH	E	NO EQUIVALENT COLOR PHOTO AS16-131-20,162
	62	10A	YES	64	" "	3750 Å	4.3	1/60	"							E	AS16-131-20,163
	63	10A	YES	65	" "	>4000 Å	4.3	1/250	"							P	AS16-131-20,164
	64	10A	YES	66	☾ DISC	>4000 Å	4.3	1/250	YES							P	AS16-131-20,165
NO. 10-B	65	10B	YES	67	☾ DISC.	3050 Å	5.6	1/60	YES							G	AS16-131-20,166
	66	10B	"	68	" "	3050 Å	5.6	1/60	"							G	AS16-131-20,167
	67	10B	"	69	" "	2600 Å	5.6	1.0	"							P	AS16-131-20,168
	68	10B	"	70	" "	2600 Å	5.6	1.0	"							P	AS16-131-20,169
	69	10B	"	71	" "	3750 Å	5.6	1/60	"	No ⊕	201:15:[illegible]	4/25/72 03-[illegible]	212,554 NM.	N/A	λ 023° 00' WEST φ 02° 56' SOUTH	G	AS16-131-20,170
	70	10B	"	72	" "	3750 Å	5.6	1/60	"							G	AS16-131-20,171

REMARKS

(Photos 49–56 and No. 6 Extra):

SEE NOTE ① AT BOTTOM OF SHEET

SEE NOTE ② AT BOTTOM OF SHEET

FRAMES 20,148 THROUGH 20,157 WAS TAKEN ON ☾ REV. No. 27 AT AN ALTITUDE OF 113 KM. THE CO-ORDINATES OF THE PRINCIPAL POINT FOR FRAME 20,154 IS:

λ 13.8° EAST
φ 7.5° SOUTH
⊙ ∠ 24°

CRATERS (MAJOR) = DOLLAND BB
DOLLAND C
DOLLAND D

(ORBITER IV SUBFRAME 84-3.

CRATERS IDENTIFIED ON PAGE 126 OF NASA-SP-[illegible], "ATLAS AND GAZETTEER OF THE NEAR SIDE OF THE MOON" BY DANNY C. KINSLER, ET AL.

(Photos 57–64): LUNAR DISC - SET 1 SEQUENCE

TRANS EARTH COAST (TEC)

(Photos 65–70): LUNAR DISC - SET 2 SEQUENCE

TEC

NOTE: ① MRD TARGETS Nos. 7, 8, & 9 DELETED FROM FLIGHT PLAN BY MSC/MISSION CONTROL.
② TARGET No. 6 WAS LISTED IN MRD LIST (AS SHOWN) TO BE LUNAR MARIA BUT IS ACTUALLY LUNAR TERRA - 10 EXP. NOT 8 PER PANORAM.

J.W.S. 8/[illegible]

SEQUENTIAL

EXPERIMENT S-177 (UVPTG ⊕ & ☾) FILM DATA - AP-16

PAGE No 4

SCHEDULED PHOTO No. MRD		TARGET No. MRD	PHOTO YES/NO	ACTUAL PHOTO No.	TARGET / SUB TEST	λ (Å) PASS BAND CENTER	f/STOP	EXPOSURE	TRUE IMAGE	IMAGE DIAM.	GET SEQUENCE TIME	GMT SEQ TIME	CM-DISTANCE FROM THE ⊕	⊙ SUB POINT	SUB-SPACECRAFT φλ AT SEQUENCE TIME	IMAGE QUAL.	AS16-FRAME No.	REMARKS
10-8	71	108	YES	73	☾ DISC	>4000 Å	5.6	1/500	YES							[illegible]	AS16 - 131 - 20,172	LUNAR DISC - SET 2 SEQUENCE
	72	108	YES	74	☾ DISC	>4000 Å	5.6	1/500	YES							[illegible]	AS16 - 131 - 20,173	TEC
	No	NONE	NO	—	NONE	—	—	—	NONE	—	—	—	—	—	—	NONE	AS16 - 131 - 20,174	BLACK - UNSCHEDULED IMAGE
NO. 11	73	11	YES	75	⊕ DISC	3050 Å	5.6	1/125	YES							G	AS16 - 131 - 20,175	⊕ VIEW COVERAGE
	74	"	"	76	" "	3050 Å	5.6	1/125	"							G	AS16 - 131 - 20,176	NORTH AMERICA, CENTRAL AMERICA, SOUTH AMERICA; HAWAII, PACIFIC AREA
	75	"	"	77	" "	2600 Å	5.6	1/5	"							P	AS16 - 131 - 20,177	TEC
	76	"	"	78	" "	2600 Å	5.6	1/1	"							P	AS16 - 131 - 20,178	
	77	"	"	79	" "	3750 Å	5.6	1/250	"	51MM	[illegible]	4/21/72 [illegible]	50,113 NM	? [illegible]	λ 143° 08' EAST φ 19° 05' [illegible]	E	NO COLOR PHOTO TAKEN AS16 - 131 - 20,179	1 SET OF ⊕ DISC (THIN CRESCENT)
	78	"	"	80	" "	3750 Å	5.6	1/250	"							E	AS16 - 131 - 20,180	CONSPICUOUS WHITE FLARE OR SPOT IN ⊕ ATMOSPHERE. POSSIBLY HIGH ALT. CLOUDS (?) FROZEN 1/8 CRYSTALS 3750Å APPEAR TO GIVE BEST DETAIL.
	79	"	"	81	" "	>4000 Å	8.0	1/500	"							MEDIUM F-P	AS16 - 131 - 20,181	LENS REFLECTIONS
	80	"	YES	82	⊕ DISC	>4000 Å	8.0	1/500	YES							MEDIUM F-P	AS16 - 131 - 20,182	

NOTE: ② BETWEEN TARGETS 10-8 & 11. (FRAMES 96 & 97) IS A SINGLE BLACK NON-SCHEDULED - NO IMAGE - FRAME.

J.W.S.
8/11/72

27

Appendix 2

Public Information

In response to written requests, over 25 copies of the Apollo 16 preliminary science report have been sent out thus far. Others have been circulated to scientists working in related areas of planetary research. The photographs have also been used as illustrations in graduate and undergraduate courses at SUNY/Stony Brook.

Fig. 1

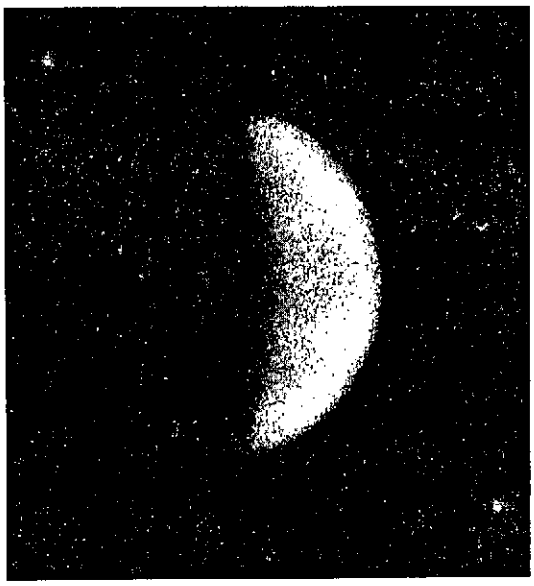

Fig. 2

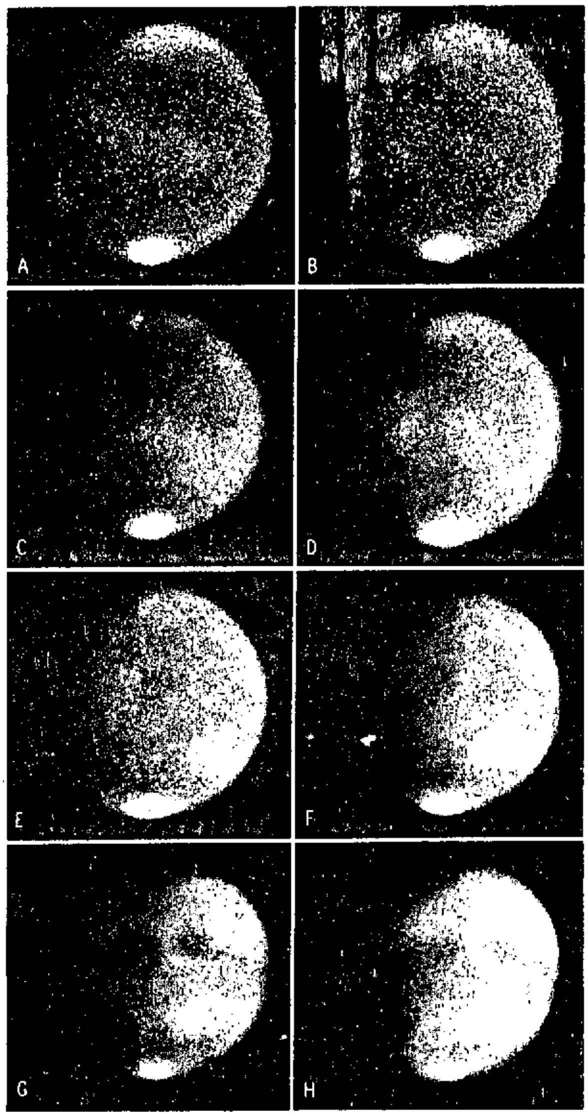

Fig. 3

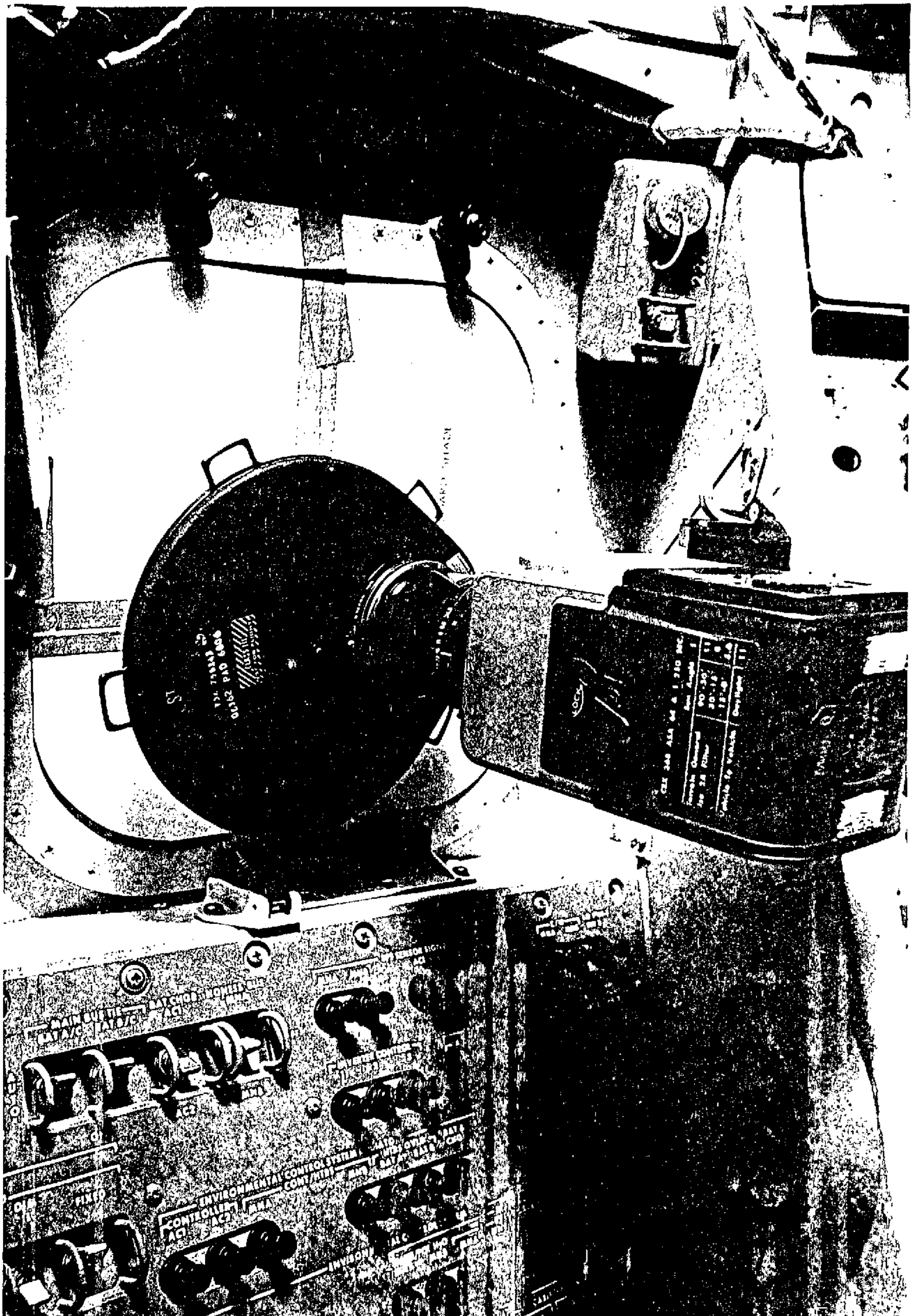

NASA
S-72-32985

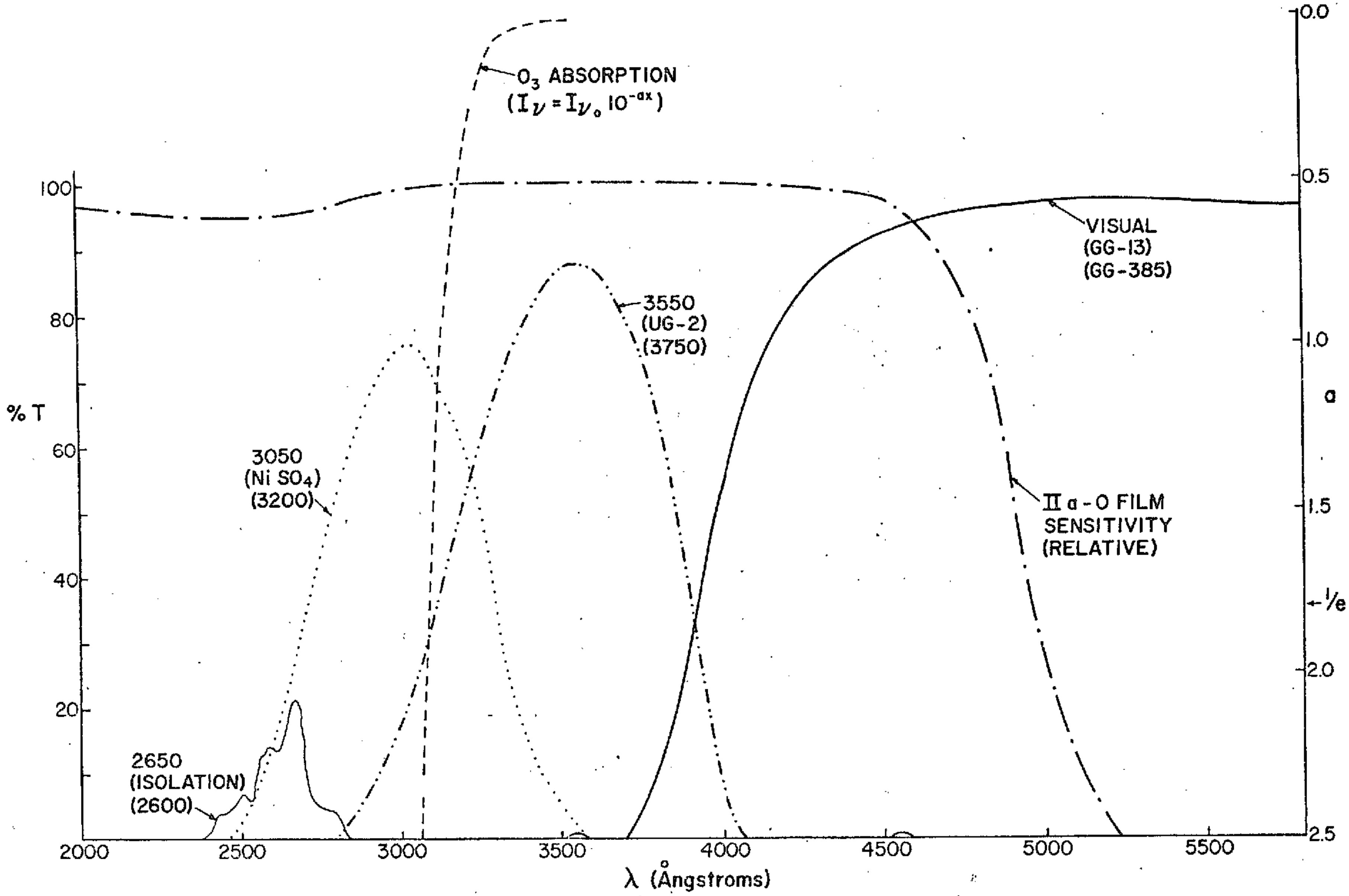

O3 ABSORPTION
($I_\nu = I_{\nu_0} 10^{-ax}$)
3550
(UG-2)
(3750)
3050
(Ni SO4)
(3200)
2650
(ISOLATION)
(2600)
VISUAL
(GG-13)
(GG-385)
II a - O FILM
SENSITIVITY
(RELATIVE)
% T
a
←1/e
100
80
60
40
20
0.0
0.5
1.0
1.5
2.0
2.5
2000
2500
3000
3500
4000
4500
5000
5500
λ (Ångstroms)

Fig. 4

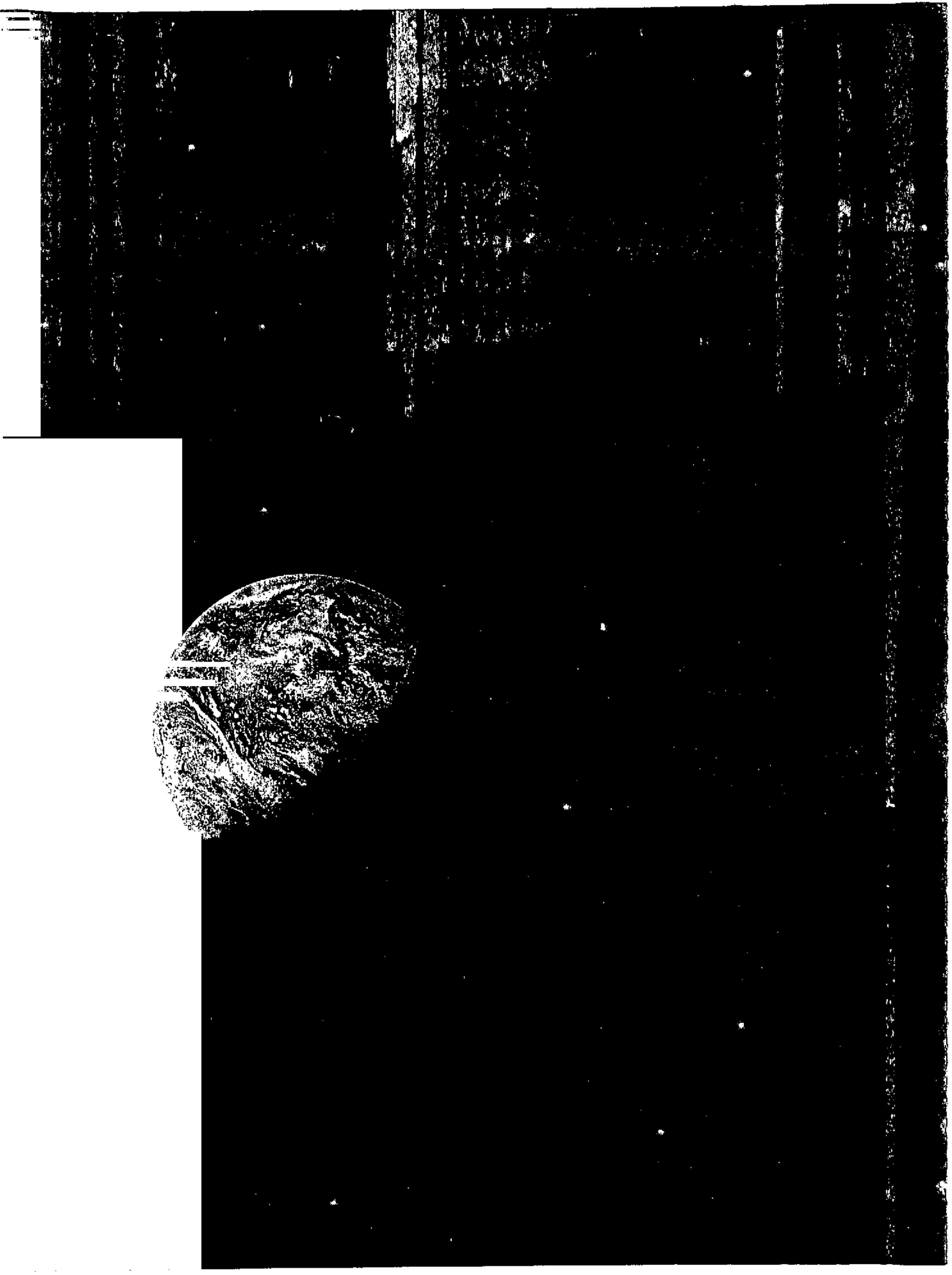

Fig. 5

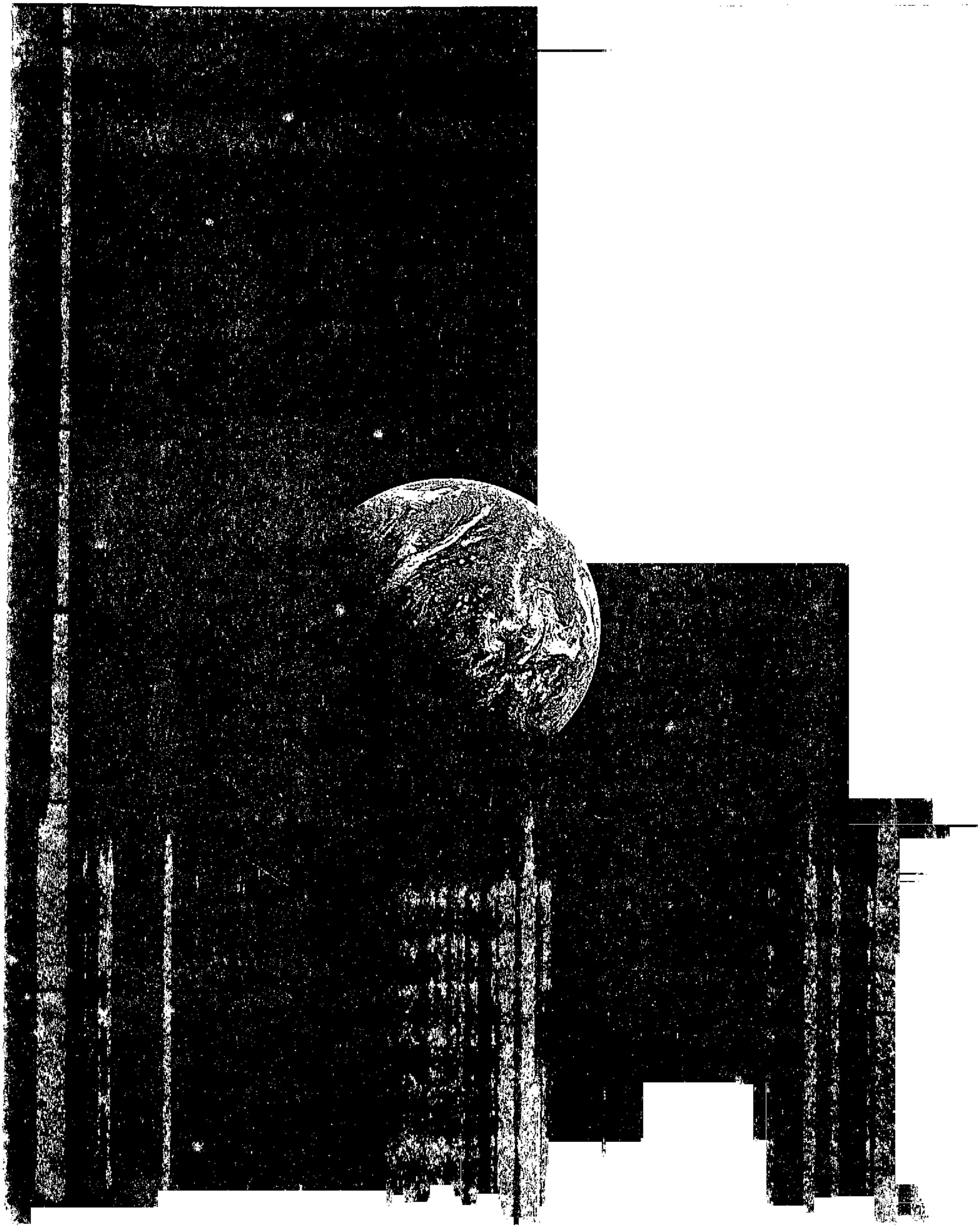

Fig. 7

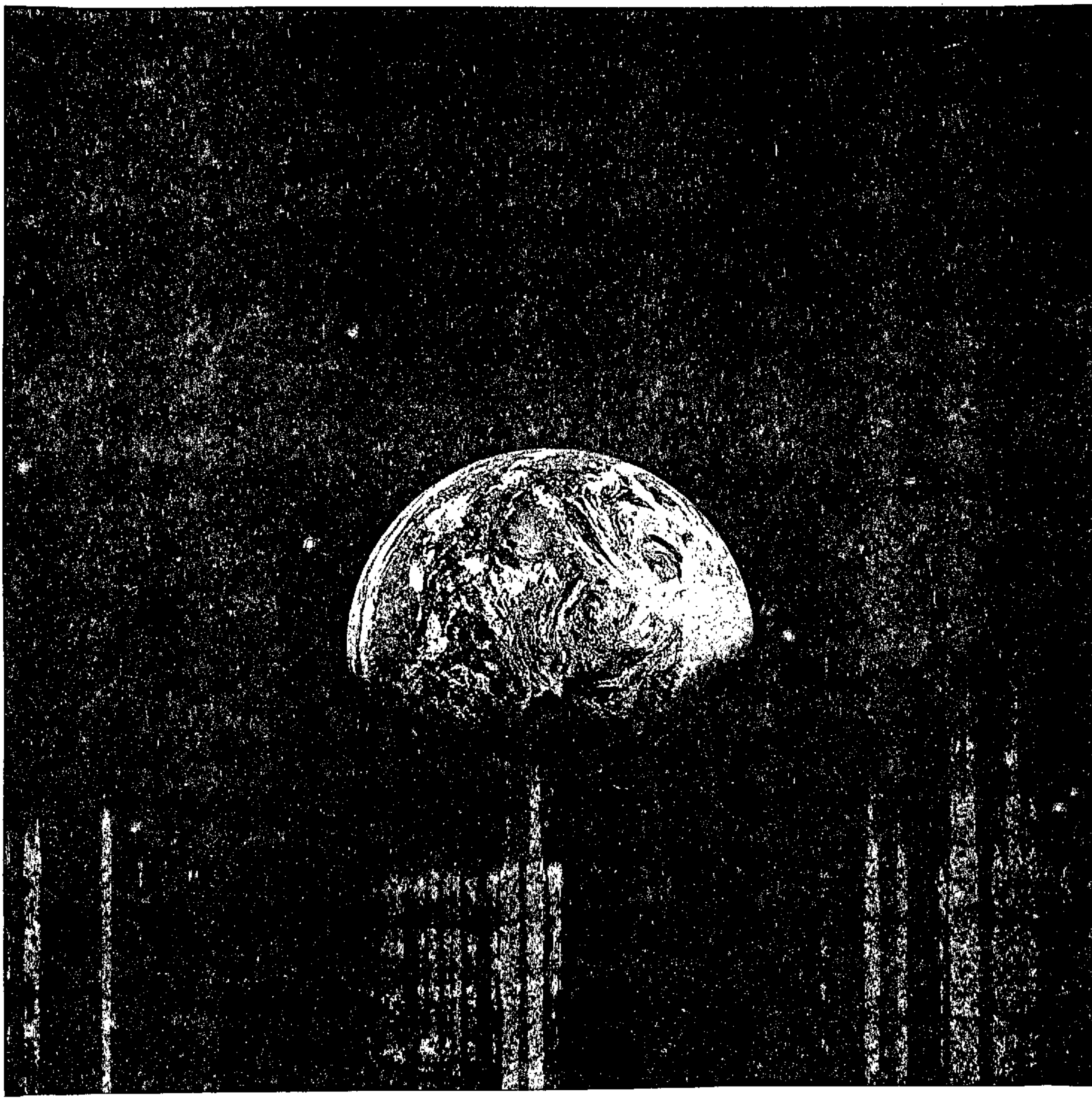

NASA AS16-131-20106

Fig. 8

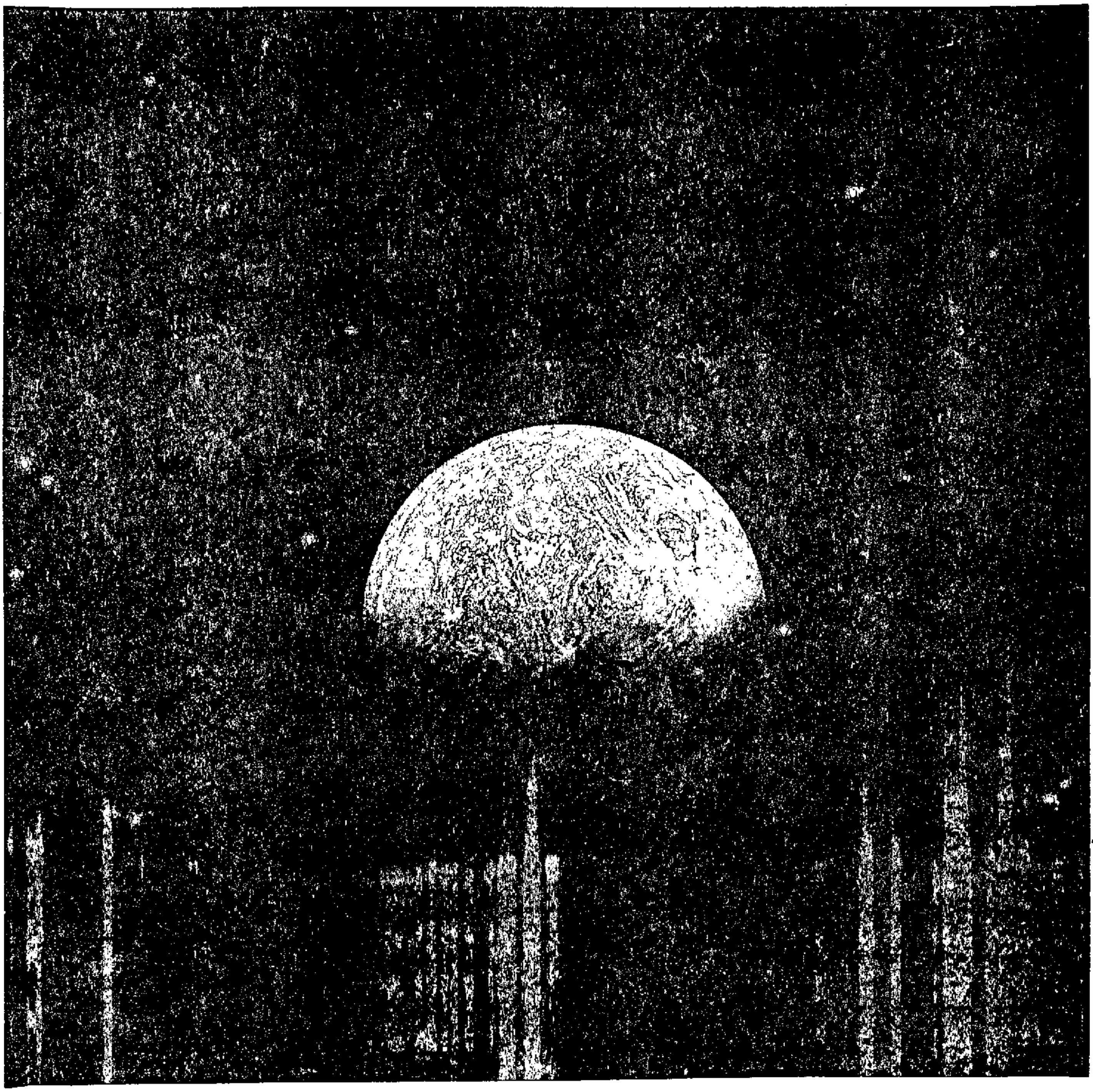

NASA
AS16-131-20100

Fig. 9

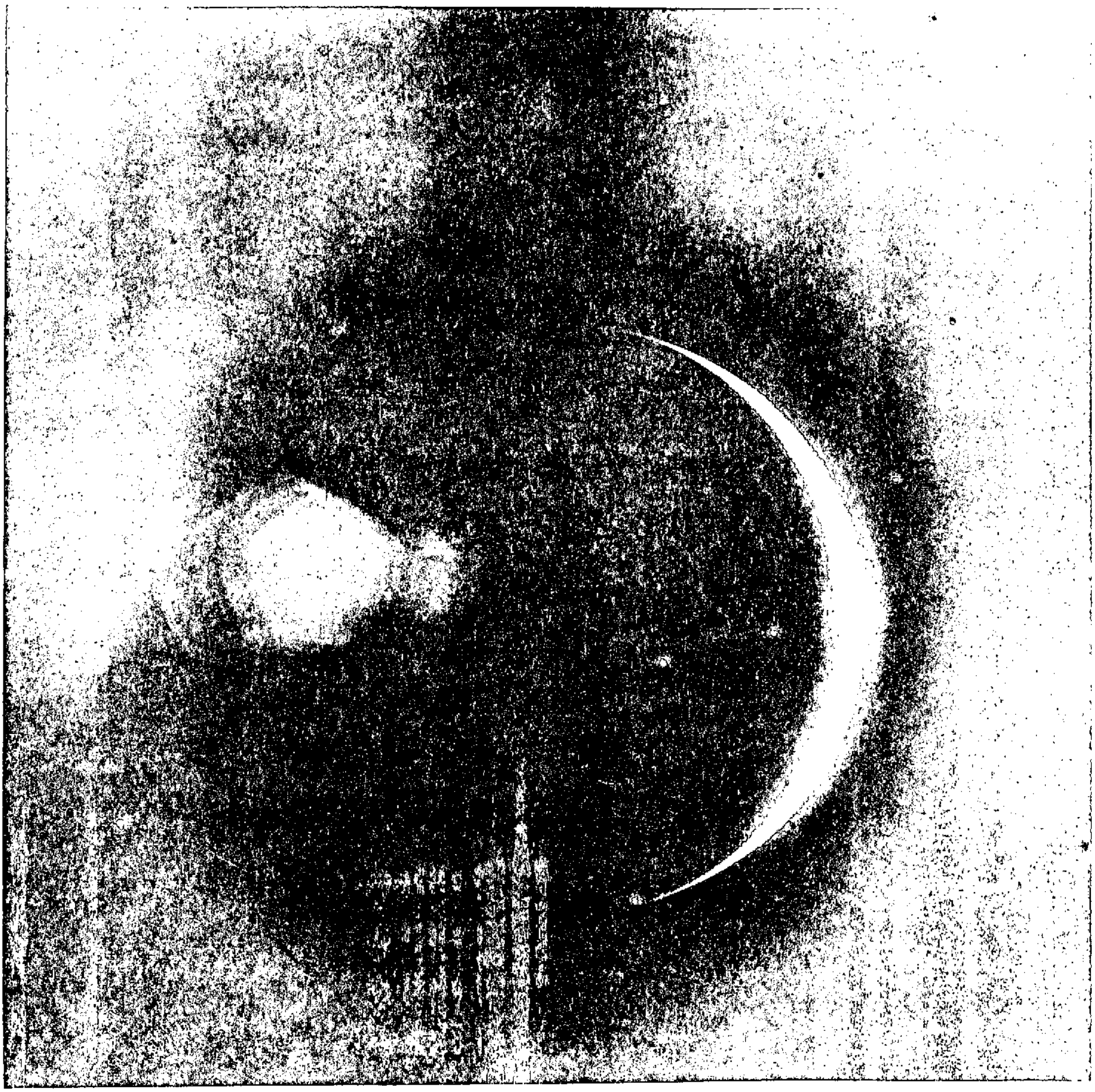

NASA
AS16-131-20181

Fig. 10

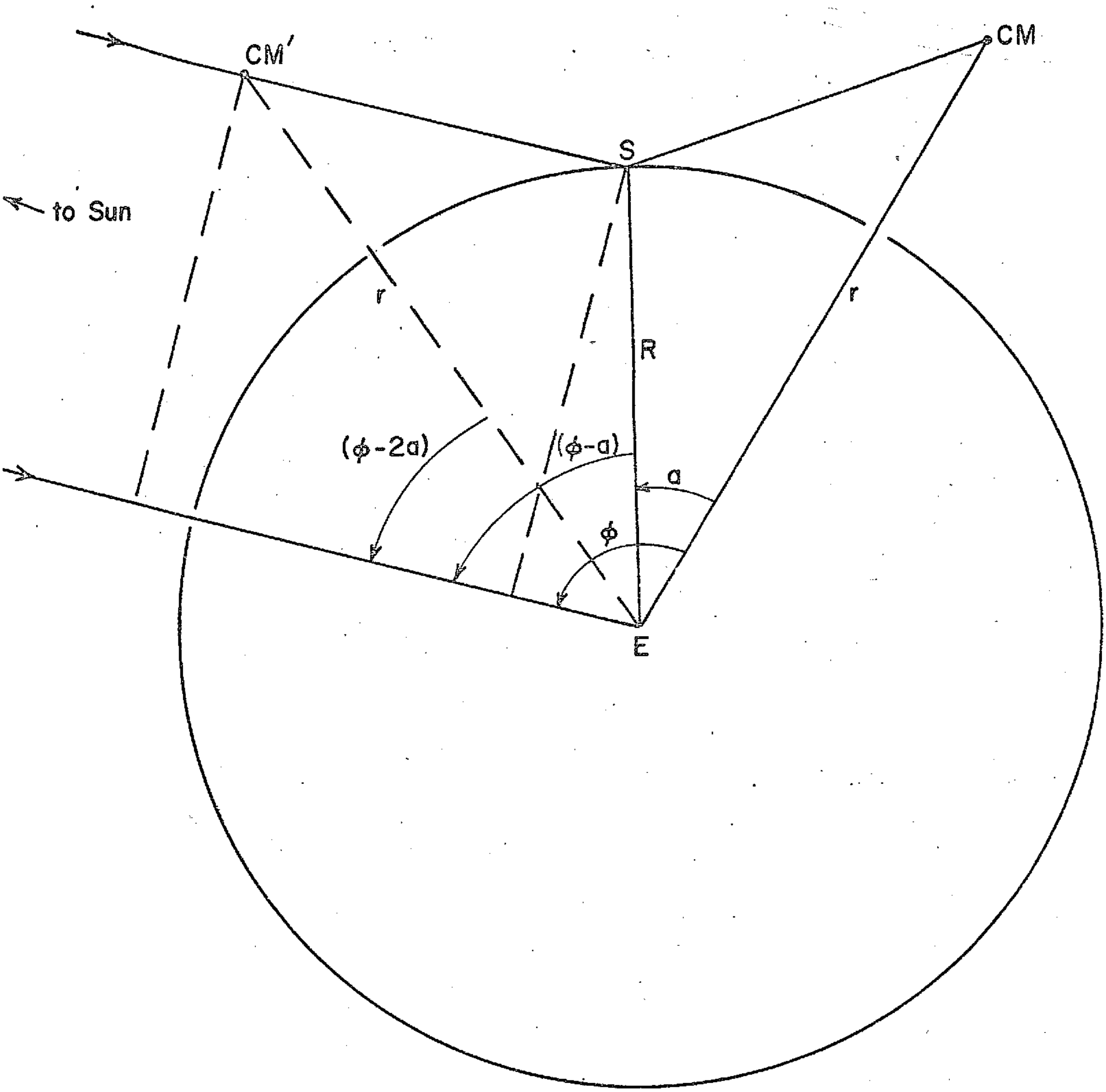

Fig. 11

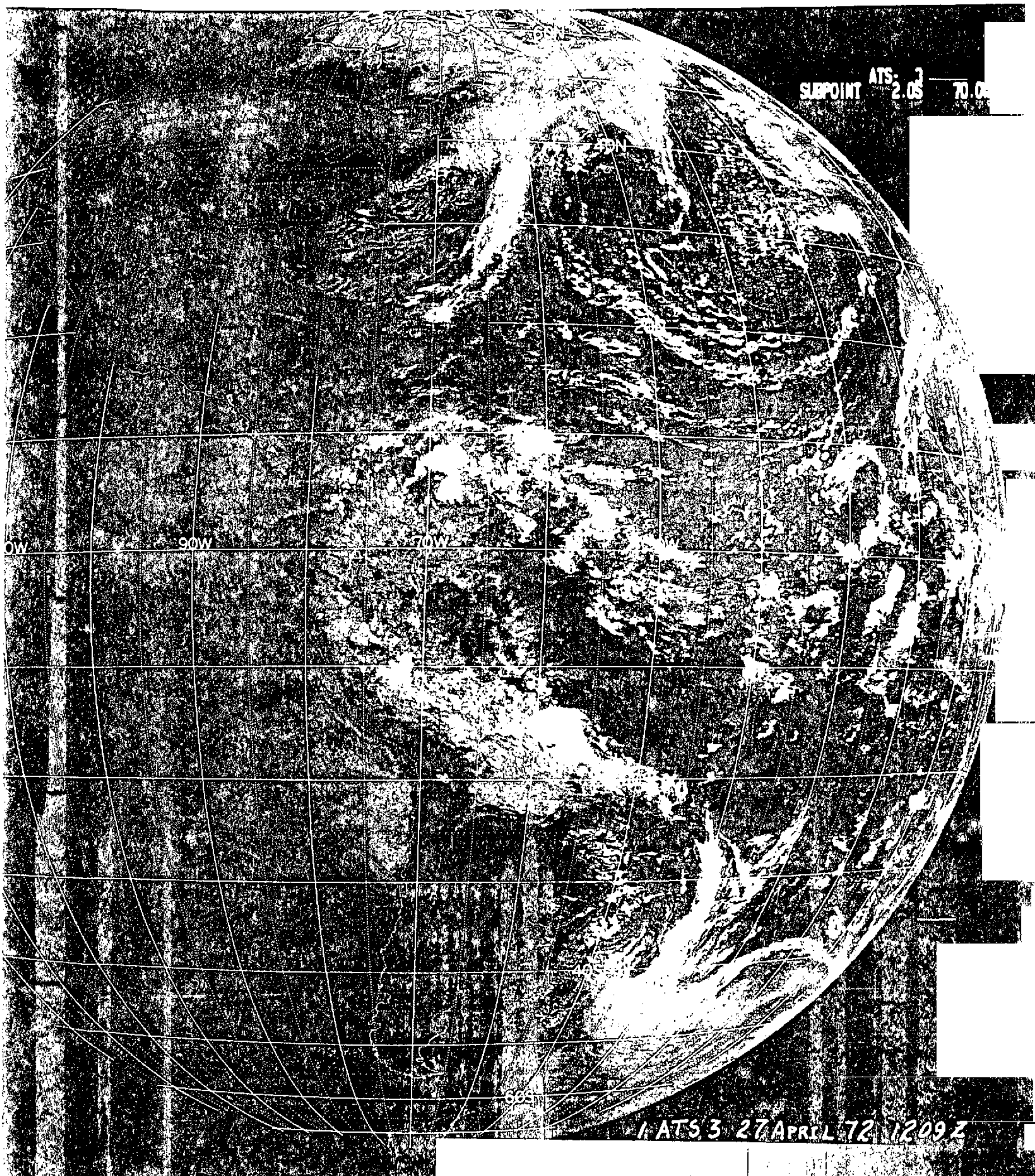

Fig. 12

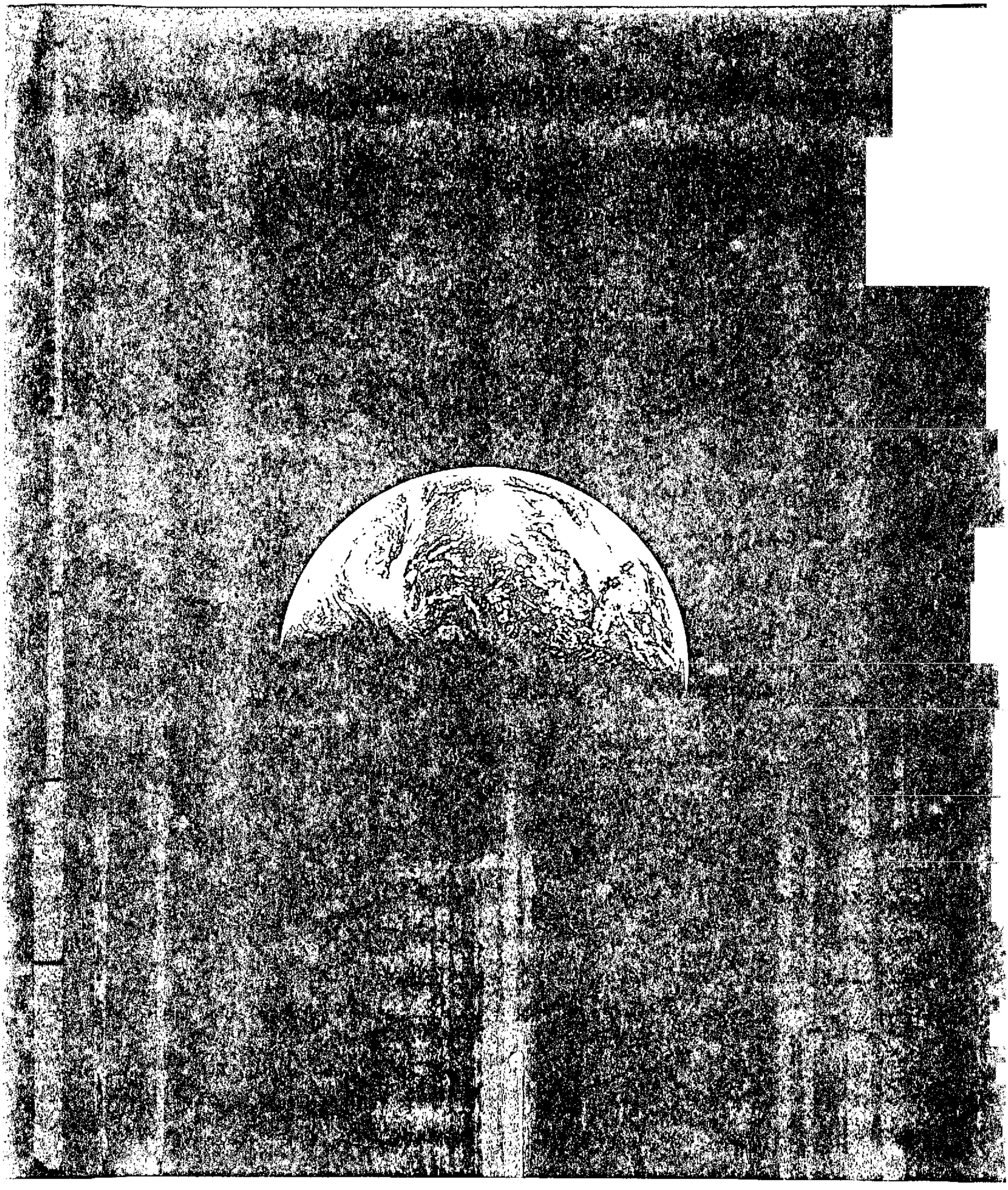

Fig. 13

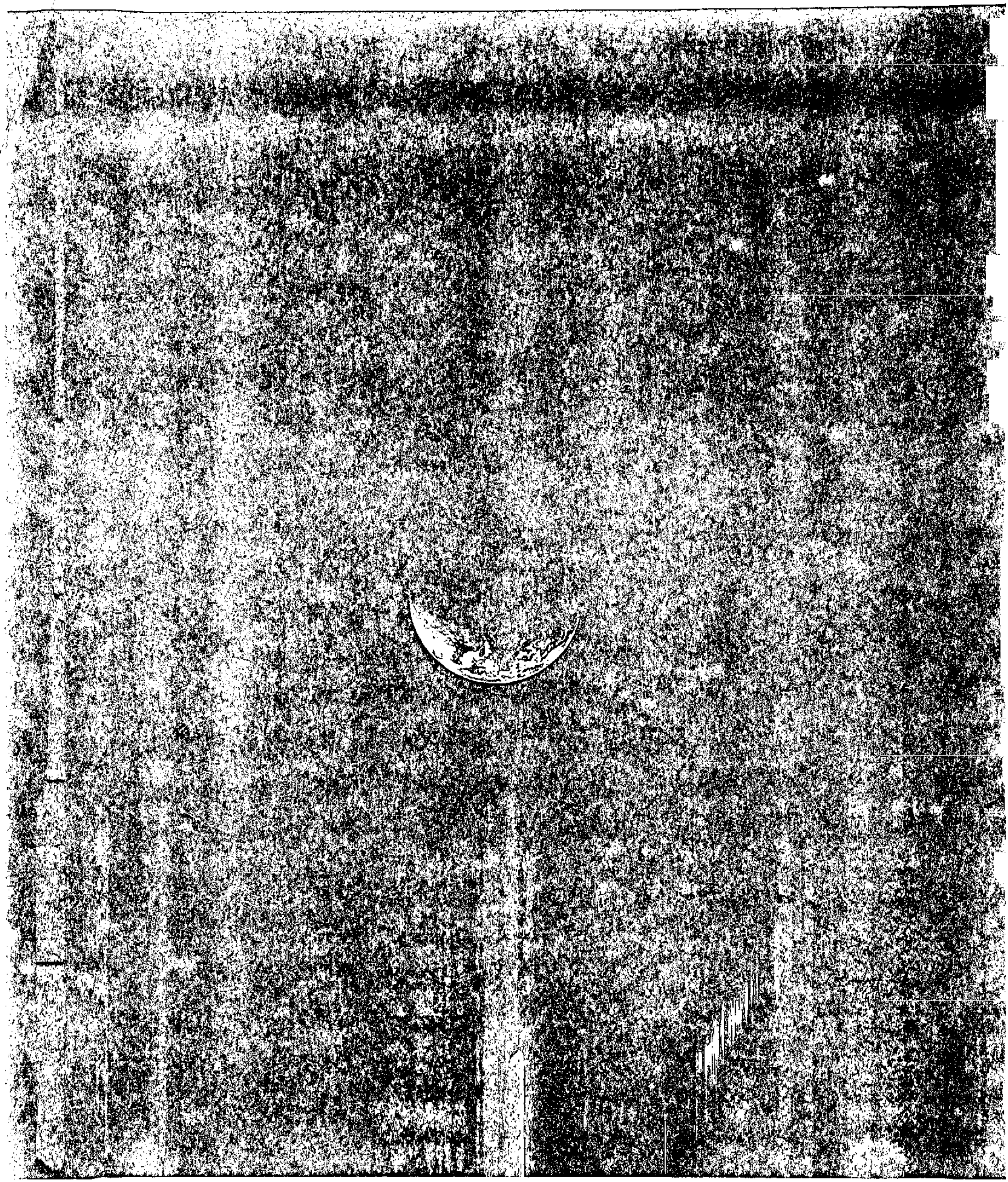

Fig. 14

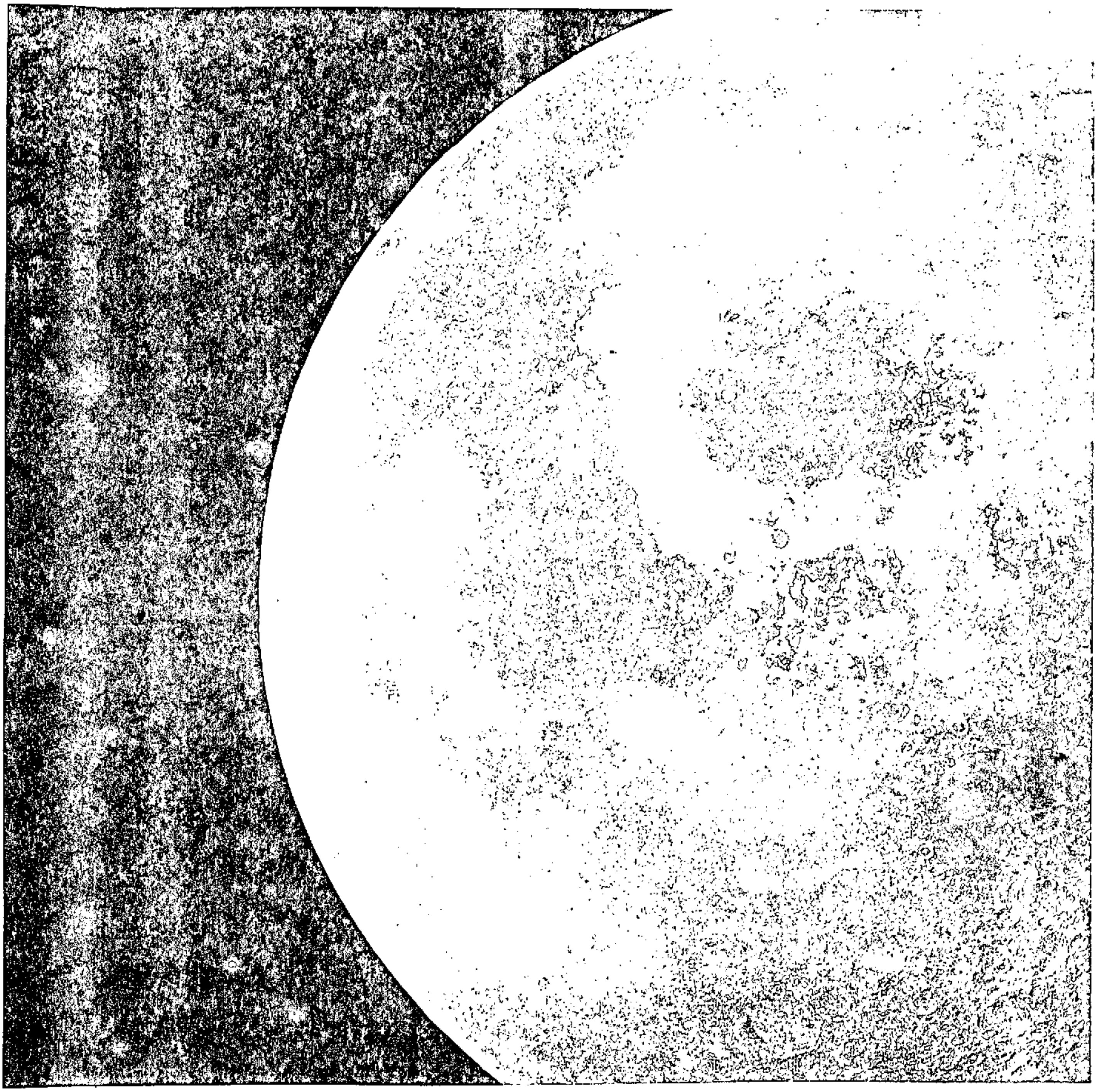

NASA
AS16-131-20165

Fig. 15

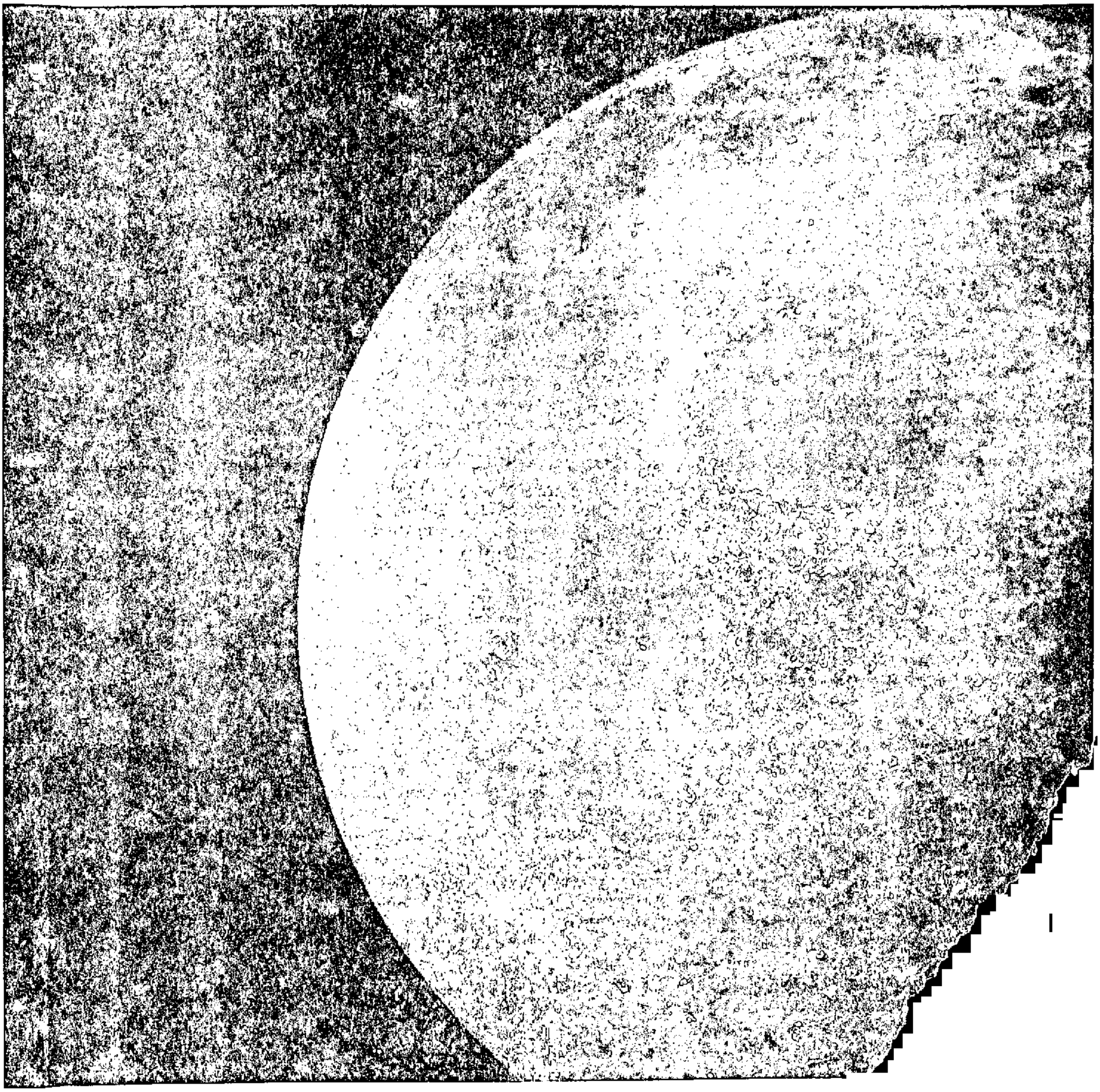

NASA
AS16-131-20158